GEODESY AND GEODYNAMICS 2015, VOL 6 NO 6, 429–436

Available online at www.sciencedirect.com

ScienceDirect

journal homepage: www.keaipublishing.com/en/journals/geog; http://www.jgg09.com/jweb_ddcl_en/EN/volumn/home.shtml

Temporal variation of gravity field prior to the Ludian Ms6.5 and Kangding Ms6.3 earthquakes

Hao Hongtao[a,b], *Wei Jin*[a,b], *Hu Minzhang*[a,b], *Liu Ziwei*[a,b], *Li Hui*[a,b,*]

[a] *Key Laboratory of Earthquake Geodesy, Institute of Seismology, China Earthquake Administration, Wuhan 430071, China*

[b] *Wuhan Base of Institute of Crustal Dynamics, China Earthquake Administration, Wuhan 430071, China*

ARTICLE INFO

Article history:
Received 12 September 2015
Received in revised form
16 October 2015
Accepted 17 November 2015
Available online 29 December 2015

Keywords:
Ludian Ms6.5 earthquake
Kangding Ms6.3 earthquake
Gravity variation
Gradient zone
Mechanism of gravity variation
Crustal movement
Deep material migration
Sichuan-Yunnan area

ABSTRACT

Using mobile gravity data from the central area of Sichuan and Yunnan Provinces, the relationship between gravity variation and earthquakes was studied based on the Ludian Ms6.5 earthquake that occurred on August 3rd, 2014, and the Kangding Ms6.3 earthquake that occurred on November 22nd, 2014; the mechanism of gravity variation was also explored. The results are as follows: (1) Prior to both earthquakes, gravity variation exhibited similar characteristics as those observed before both the Tangshan and Wenchuan earthquakes, in which typical precursor anomalies were positive gravity variation near the epicenter and the occurrence of a high-gravity-gradient zone across the epicenter prior to the earthquake. (2) A relatively accurate prediction of the occurrence locations of the two earthquakes was made by the Gravity Network Center of China (GNCC) based on these precursor anomalies. In the gravity study report on the 2014 earthquake trends submitted at the end of 2013, the Daofu-Shimian section at the junction of the Xianshuihe and Longmenshan fault zones was noted as an earthquake-risk region with a predicted magnitude of 6.5, which covered the epicenter of the Kangding Ms6.3 earthquake. In another report on earthquake trends in southwestern China submitted in mid-2014, the Lianfeng, Zhaotong fault zone was also classified as an earthquake-risk region with a magnitude of 6.0, and the central area of this region basically overlapped with the epicenter of the Ludian Ms6.5 earthquake. (3) The gravity variation characteristics are reasonably consistent with crustal movements, and deep material migration is likely the primary cause of gravity variation.

* *Corresponding author*. Key laboratory of Earthquake Geodesy, Institute of Seismology, China Earthquake Administration, Wuhan 430071, China.
E-mail address: lihuieq@163.com (Li H.).

Peer review under responsibility of Institute of Seismology, China Earthquake Administration.

Production and Hosting by Elsevier on behalf of KeAi

http://dx.doi.org/10.1016/j.geog.2015.12.004
1674-9847/

1. Introduction

On August 3rd and November 22nd of 2014, the Ludian Ms6.5 and Kangding Ms6.3 earthquakes occurred, respectively, both in the central Sichuan-Yunnan area. The two earthquakes were separated in time and space by only approximately three months and 400 km, respectively. Studies of their source rupture processes and seismogenic structures indicated that the Ludian Ms6.5 earthquake occurred on the southern border of the Daliangshan sub-block that adjoins the Bayan Har block, and its seismogenic fracture was the Baogunao-Xiaohe fault which is a secondary fault of the Lianfeng, Zhaotong fault zone [1], with its focal mechanism being a strike slip [2,3]; the Kangding Ms6.3 earthquake occurred on the eastern border of the Bayan Har block, and its seismogenic fracture was the Selaha segment of the Xianshuihe fault [4], with its focal mechanism being mainly strike strip [5]. Based on observation data of seismic waves, the gravity field, and geomagnetic field, researchers have studied physical properties such as crustal velocity structure and density structure within the two earthquake regions and their peripheral areas, and their results indicate significant differences in the structures of the two earthquakes [6–8]. These findings are useful for understanding the seismogenic environment and the mechanism of the two earthquakes; however, studies on the processes of the earthquake development and occurrence are still inadequate.

Gravity variation contains rich information about crustal movement [9–12]. Based on the surface gravity variation data from seismic gravity measurements, researchers in China recently achieved satisfactory results in predicting occurrence trends, and particularly locations, of a series of medium to large earthquakes such as the 2008 Wenchuan [13–15], 2009 Yao'an [16], and 2013 Lushan earthquakes [17]. This progress indicates the unique role of gravity variation information in understanding the development and occurrence of earthquakes. This work investigated the evolution of a gravity field during the course of the Ludian Ms6.5 and Kangding Ms6.3 earthquakes by using recent gravity measurements in the central Sichuan-Yunnan area, in order to provide insights into the seismogenic mechanism and regional tectonic setting.

2. Data and processing

The Sichuan-Yunnan area has consistently been one of the most important regions for surface gravity monitoring in China. Since 2010, the old gravity monitoring stations in this region have been upgraded and optimized into an integral monitoring network. Considering the need to study gravity variation at the epicenter and on the borders of the adjoining major blocks for both the Ludian and Kangding earthquakes, observation data were selected from the spatial dimensions of 24–32°N and 99–106°E within the time period from 2013 to 2015; there were a total of 5 integrated observation data sets for the different periods. All of the data are summarized in Table 1, and the gravity monitoring network and its monitoring regions are illustrated in Fig. 1.

In the data processing, we first performed a systematic assortment of gravity data, thus unifying the identification numbers of the monitoring stations. Then, the collected absolute gravimetry data were calibrated to remove the effects of water loads using a classical theory on surface loads [18] and GLDAS hydrological model data. The resultant data were linearly fitted to yield the gravity value within each observation period for every absolute gravity monitoring point. These gravity values subsequently served as the reference data and controlling points for the observed relative gravimetry data. Next, we carried out overall adjustment calculations over the relative gravity data and reference data according to the classical adjustment method. The error equations for the relative gravity data and reference data are as follows:

$$v_{ij} = \left(\overline{g}_j - \overline{g}_i\right) - \left(g_j - g_i\right) + E_1\left(g_j - g_i\right) - D\left(t_j - t_i\right) \tag{1}$$

$$v_h = \widetilde{G}_h - G_h \tag{2}$$

where g_i and g_j are the pre-processing gravity values at any two points i and j; t_i and t_j are the observation times at i and j; E_1 is the linear term in scale parameter of the relative gravimeter; D is the drift rate of the relative gravimeter; $\overline{g}_i$ and $\overline{g}_j$ are the unknown gravity values at the two points i and j; $\widetilde{G}_h$ is the gravity value at point h after adjustment, which is an unknown quantity for the solution here; G_h is the known gravity value from reference data; and ν_h is the adjustment correction.

The relative gravity data were subjected to solid tide correction, barometer correction, and instrument elevation correction in the adjustment calculations. In addition, in order to eliminate or minimize the disturbance caused by systematic errors of the instruments, scale parameters of the relative gravimeters were calculated using the absolute gravity observations as the controlling points. The treatment results indicated an average precision within 15×10^{-8} ms^{-2} for the gravity value at all points in each period. Finally, robust least squares collocation was applied to filter the observation data in the gravity variation mapping, in an attempt to further reduce the effects of gross errors and

Table 1 – Summary of gravity data.

Observation period	Relative gravity data	Absolute gravity data	
	Observation time	Monitoring station	Observation time
2013, First half	2013.04–07	Pixian, Luzhou, Dongchuan, Xichang, Ganzi	2013.06–07
2013, Second half	2013.08–11	N/A	
2014, First half	2014.03–05	Pixian, Luzhou, Guangyuan, Xiaguan, Kunming, Xichang, Ganzi	2014.01–06
2014, Second half	2014.08–10	Pixian, Kunming, Xiaguan, Lijiang, Xichang, Ganzi	2014.06–10
2015, First half	2015.02–05	Pixian, Kunming, Xiaguan, Lijiang, Xichang, Ganzi	2015.02–06

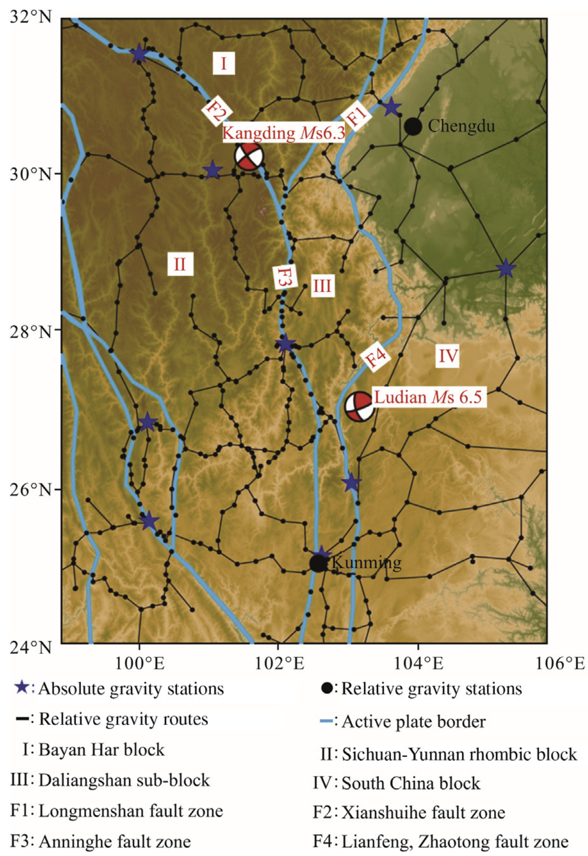

Fig. 1 – Spatial distribution of the observed gravity data.

shallow surface defects, and highlight the gravitational effects of the tectonic features.

3. Results and analysis

The differential and cumulative gravity variation patterns of the study area from 2013 to the first half of 2015 are shown in Figs. 2 and 3, respectively. The differential pattern shows the variation between adjacent observation periods (on a half-year scale), which is used to reveal the differences in the dynamic evolution of the gravity field between the different periods. The cumulative pattern presents the variational results relative to the observations in the first half of 2013, which focuses on the cumulative effects over a long term.

3.1. *Differential gravity variation*

2013.05–2013.10 (Fig. 2a): noticeable changes occurred in the northern part of the gravity network region. Bordering on the west side of the Longmenshan Fault, the western Sichuan plateau mostly showed a positive anomaly, with a maximum magnitude greater than 110 μGal. On the east side, the Sichuan Basin was characterized by highly negative anomalies, with a maximal anomaly on the order of −60 μGal. The Longmenshan Fault formed a sharp boundary dividing the regions of positive and negative anomalies, developing a high gradient zone with a gravity difference bigger than 120 μGal. The Kangding *Ms*6.3 earthquake occurred right at the extending and bending location of this high gradient. The southern part of the gravity network had relatively gentle variation, being mostly low and positive. Further analyses of the overall pattern of the gravity variation in this period indicated a zero-value region that extended along the Longmenshan-Anninghe-Zemuhe-Lianfeng-Zhaotong fault zone. This suggests that the main tectonic features in this area governed the distribution of gravity variation in this period.

2013.10–2014.05 (Fig. 2b): in this period, the overall gravity variation changed from positive in the northeast to negative in the southwest. Positive anomalies occurred mainly within the Sichuan Basin and Daliangshan sub-block, and intruded toward the southwest into the sichuan-yunnan rhombic block, with a maximum magnitude of approximately 50 μGal. In comparison with the last period, the positive region roughly shifted toward the southeast from the western Sichuan plateau. Meanwhile, the Longmenshan Fault and the Lianfeng, Zhaotong fault zone clearly played a role in controlling its boundaries. The south of Zhaotong was a region of highly negative anomalies with a maximum order of 90 μGal. As a result, the Lianfeng, Zhaotong fault zone became the most distinct gradient zone with the sharpest variation and the dividing boundary between positive and negative anomalies (with a gravity difference on the order of approximately 90 μGal). The Ludian Ms6.5 earthquake occurred right within this high gradient zone. The distribution of gravity variation isolines around Longmenshan indicated a weak gradient zone with approximately 30 μGal gravity difference in this area.

2014.05–2014.10 (Fig. 2c): in comparison with the last period, the overall gravity variation showed an opposite trend with an evidently decreased magnitude in its variation. Except for Anlong, which had a local positive anomaly up to approximately 60 μGal, the remaining areas had variations that ranged between +30 and −30 μGal. The south of Zhaotong-Luzhou was a region of positive anomalies with relatively high magnitude, and the largest gradient in gravity variation in this period occurred within the Lianfeng, Zhaotong fault zone and its northeast extensional region. When compared with the last period, the positive region shifted toward the southeast. Once again, the Lianfeng, Zhaotong fault zone governed the boundaries of the region. The overall variation appeared relatively gentle in the north of the gravity network region, and the Kangding Ms6.3 earthquake occurred on the zero isoline that extended southwest from Ganzi.

2014.10–2015.05 (Fig. 2d): in this period, the gravity variation appeared gently and discretely distributed with a quasi-uniform fashion. The variation values were within the range of ±30 μGal across the entire region. The Xinduqiao area, Yanyuan area and east of Kunming had relatively high values of gravity variation, which assumed a discrete distribution, whereas the gradient zone disappeared along the Zhaotong-Luzhou area.

3.2. *Cumulative gravity variation*

2013.05–2013.10 (Fig. 3a): Same as above.

2013.05–2014.05 (Fig. 3b): Compared with the last period, the overall gravity variation was intensified in the north and weakened in the south. The positive anomalies in the western

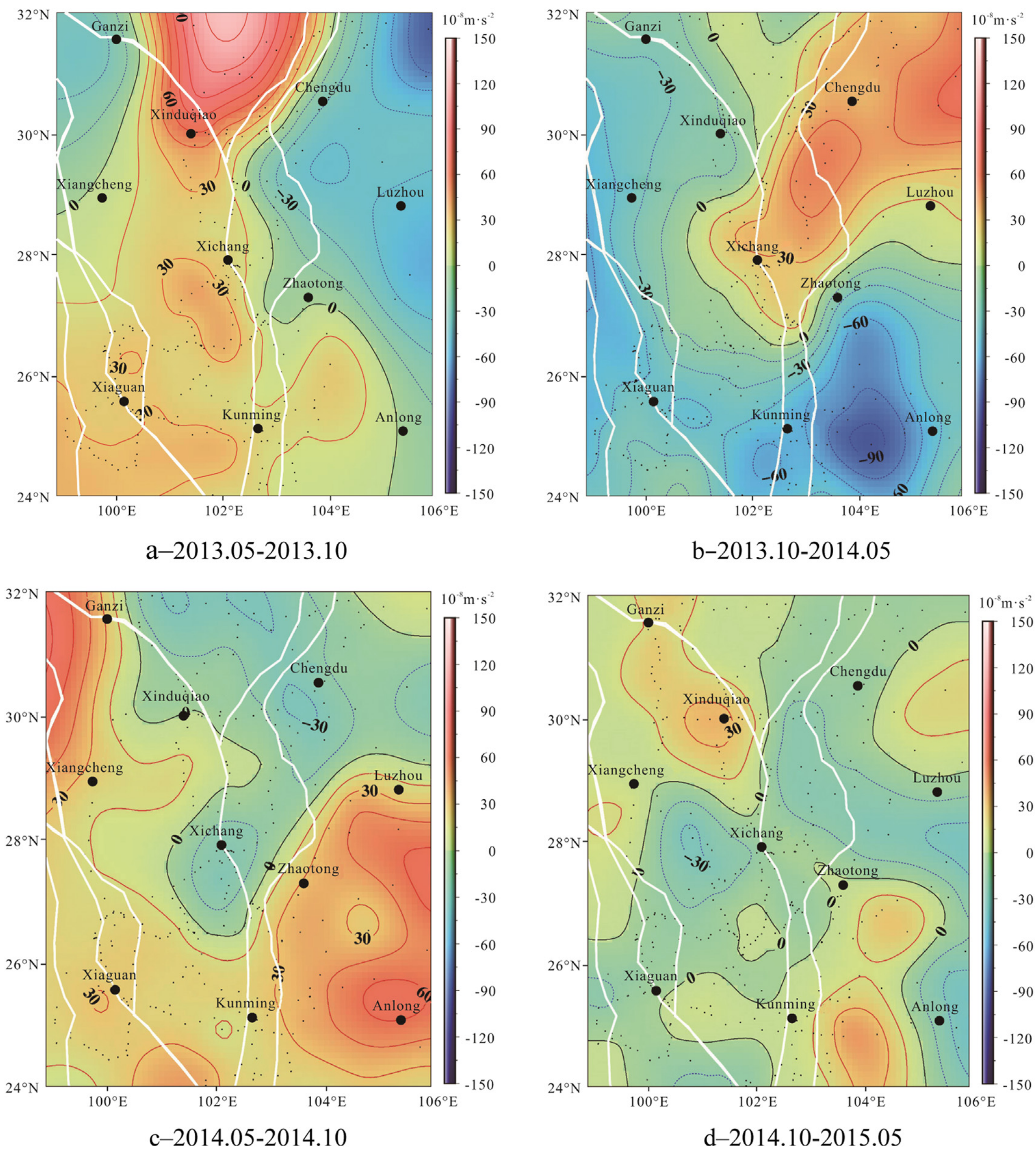

Fig. 2 — Differential gravity variation.

Sichuan plateau and Xichang area were increased by approximately 20–30 μGal, while the negative variation in the Sichuan Basin changed into low and positive variation, with a noticeable gradient zone developed near the Longmenshan area. On the contrary, the southern part of the network region changed from positive to negative variation, with maximum negative anomalies up to 60 μGal occurring in the south of the Zhaotong-Luzhou areas. The trend of the isolines near Zhaotong exhibited a 90° deflection from the north-west direction in the last period, and the variation magnitude increased considerably, forming a high gradient zone and a positive–negative transition zone that was similar to the Lianfeng, Zhaotong faults. The Ludian Ms6.3 earthquake only occurred on the zero isoline within this gradient zone.

2013.05–2014.10 (Fig. 3c): the gravity variation pattern was similar to that in the last period. The overall variation magnitude became weaker to some extent, so that the positive anomalies in the western Sichuan plateau and the high gradients in the peripheral areas even stood out. The positive variation tended to be more dispersed in the Xichang area, and the gradient decreased in the Zhaotong area, which both suggest that tectonic activities in this region became slightly weaker after the Ludian *Ms*6.5 earthquake. The positive variation in the western Sichuan plateau decreased in magnitude by roughly 20 to 30 μGal, and the Sichuan Basin transitioned to a region with negative variation. However, the gradient zone was retained along the Longmenshan Fault. The Kangding *Ms*6.3 earthquake occurred on the westward extension of the gradient zone where it intersected with the Xianshuihe Fault.

2013.05–2015.05 (Fig. 3d): in comparison with the last period, the positive anomalies in the western Sichuan

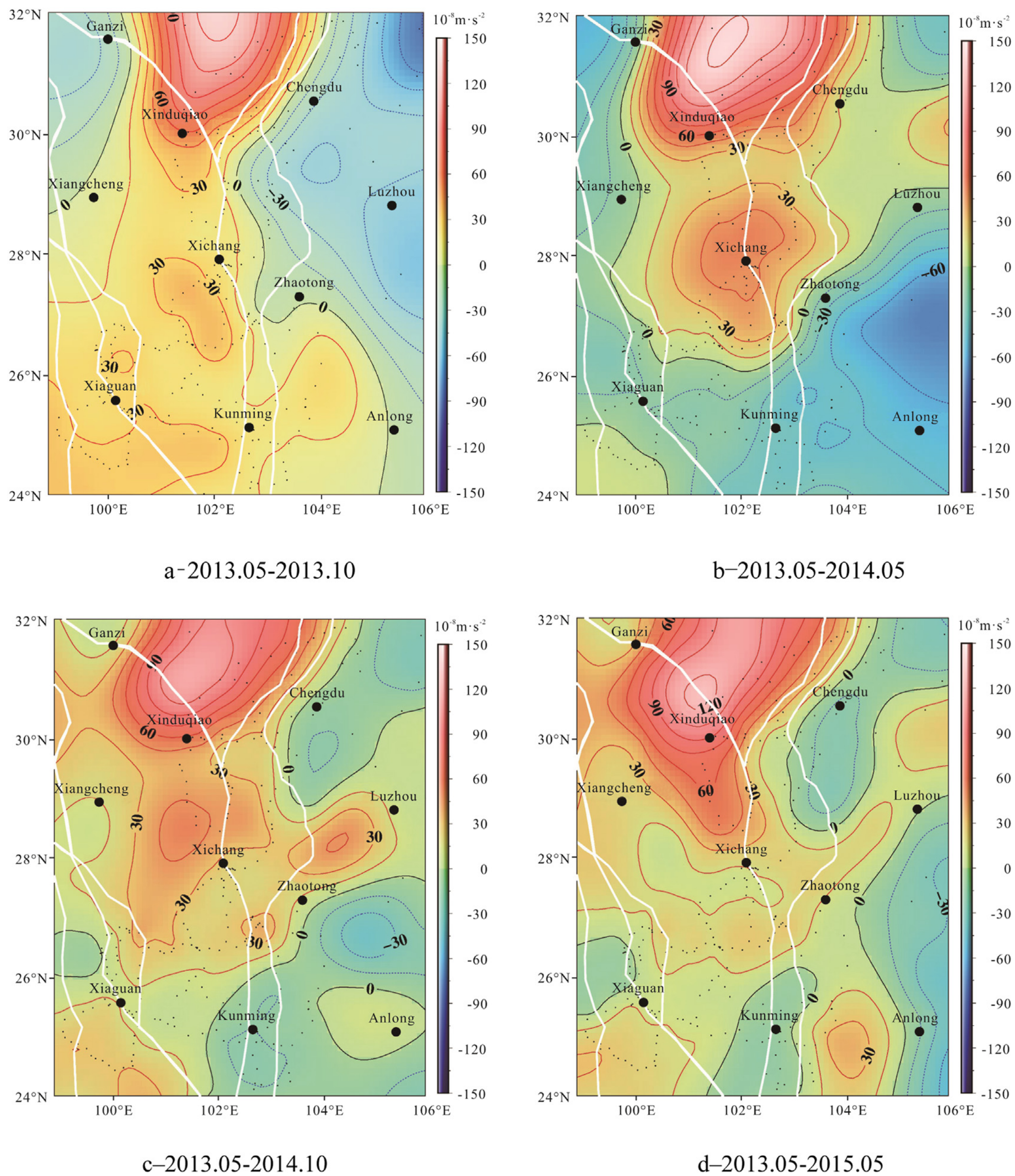

Fig. 3 – Cumulative gravity variation.

plateau were intensified again by approximately 20–30 μGal, and this positive-anomaly region expanded toward the south with the Anninghe Fault being the east boundary. The Longmenshan-Anninghe fault zone was evidently a gradient zone. The gravity variation in the south-central part of the study area continued to weaken, with gravity difference in the Zhaotong area being further weakened.

4. Gravity variation and earthquake activities

Surface gravity variation is closely related to earthquake activities. Chen et al. [19] and Li et al. [20] investigated the gravity variation before and after the Tangshan earthquake, and their results indicated a significant increasing trend in the gravity field of the earthquake region prior to the earthquake. These authors attributed the gravity variation primarily to Moho uplift that was caused by the upwelling of hot material. Shen et al. studied the precursor features of gravity variation in the Yutian earthquake [21] and the Wenchuan earthquake [13], and their results further confirmed the significance of positive anomalies in indicating the development and occurrence of earthquakes. They also pointed out that positive anomalies favor continuous buildup of seismic energy, and high gradient zones of differential variation favor shear fracturing of earthquakes. Zhu et al., who studied the major strong earthquakes that recently occurred on the mainland of China [14,15,22,23], thought that gravity variation consistent with regional tectonics in their distribution is usually a reflection of tectonic activity elements. Large earthquakes commonly occur in gradient zones and positive–negative transition zones that overlap with tectonic distribution, and transitional changes and isoline reversals in gravity-field evolution are likely precursor anomalies prior to earthquakes.

Analyses of the gravity variation above led to the following general results. (1) Positive anomalies usually play a leading role. They generally concentrate in space and have greater magnitudes than negative anomalies. The Ludian *M*s6.5 and Kangding *M*s6.3 earthquakes both occurred at the margin of positive-anomaly regions. In the differential gravity variation patterns, the positive-anomaly regions continued shifting southeast, and after migration to the Daliangshan sub-block, the Ludian *M*s6.5 earthquake occurred on its southern border. In the pre-seismic pattern of the Kangding *M*s6.3 earthquake (Fig. 2c, 2014.05–2014.10), the epicentral region had no noticeable anomalies, and the seismic location was on the zero isoline dividing the positive and negative anomalies. In contrast, the north of the earthquake region showed continual high anomalies in the cumulative patterns. (2) The Longmenshan Fault and the Lianfeng, Zhaotong faults obviously had controlling effects in the gravity variation patterns, which are closely related to tectonic distribution. In the differential patterns, the positive variation regions under shift always bordered the Longmenshan Fault and the Lianfeng, Zhaotong fault zone, and the fault zone always showed high-gradient features clearly. In the pre-seismic pattern (Fig. 2b, 2013.10–2014.05), the Ludian earthquake took place right on the zero isoline in the gradient zone that overlapped with the Lianfeng, Zhaotong fault zone, and the isoline had a 90° deflection in its trend compared with the last period. In the cumulative variation patterns, high gradient zones and positive–negative transition boundaries remained along the Longmenshan Fault, and the Kangding *M*s6.3 earthquake occurred at the extending and bending part of the gradient zone. The high gradient zone also appeared along the Lianfeng, Zhaotong faults prior to the Ludian earthquake (Fig. 3b, 2013.05–2014.05), and the epicenter of the Ludian earthquake was also on the zero isoline in the gradient zone. After the earthquake, the differential variation tended to weaken. (3) The characteristics of gravity variation prior to both the Ludian *M*s6.5 and Kangding *M*s6.3 earthquakes are essentially consistent with those from studies of the Tangshan and Wenchuan earthquakes, which both pointed to “precursor anomalies” in gravity that were likely induced by crustal deformation and material migration during the development and occurrence of these earthquakes.

Based on these gravity variation characteristics, Gravity Network Center of China (GNCC) made considerable progress in the practical prediction of the two earthquakes. In the gravity study report on the 2014 earthquake trends submitted at the end of 2013, the Daofu-Shimian section at the junction of the Xianshuihe and Longmenshan fault zones was noted as an earthquake-risk region with a predicted magnitude of 6.5, which covered the epicenter of the Kangding *M*s6.3 earthquake. In another report on earthquake trends in southwestern China submitted in mid-2014, the Lianfeng, Zhaotong fault zone was also considered as an earthquake-risk region with a magnitude of 6.0, and the central area of this region basically overlaps with the epicenter of the Ludian *M*s6.5 earthquake. However, in the 2015 earthquake trend report submitted at the end of October 2014, the risk region originally in the Daofu-Shimian area was moved to the Anninghe-Zemuhe fault zone, considering that the Songpan-Ganzi block between Xianshuihe and Longmenshan was impacted by the 2013 Lushan *M*s7.0 strong earthquake and the latest differential pattern (2014.05–2014.10) showed no appreciable anomaly in this area. As a consequence, the Kangding earthquake was unfortunately not predicted. Nevertheless, the foregoing analyses showed that spatial and temporal gravity variation are important for studying the development and occurrence of strong earthquakes and even predicting the occurrence, and particularly the locations, of earthquakes. Further, our results indicated an ongoing intensification of the positive anomalies in the western Sichuan plateau after the Kangding *M*s6.3 earthquake. Therefore, follow-up attention should be paid to the seismic conditions in this region in the future.

5. Discussion on the mechanisms of gravity variation

Surface gravity variation can be caused by various factors, which are principally those related to tectonic activities, including the vertical motion of the crust and variation in deep material distribution, after environmental effects such as atmosphere and water loads are removed. This work took atmospheric effects into consideration in the data processing, and eliminated or minimized the influences of water loads by using corrections of the reference data. Therefore, the subsequent information obtained for the gravity variation reflected only tectonic factors. Currently, high-precision data on crustal vertical movements are mostly acquired from leveling observations, which have drawbacks related to their long observation periods and asynchronicity with respect to gravity observations. Consequently, gravitational effects induced by crustal vertical movement can be evaluated using only a rough approximation. Wang et al. [24] used multiple periods of leveling observations in Sichuan Province and its peripheral areas between 1970 and 2006 to obtain vertical deformation information. Their results revealed the fastest vertical motion of the crustal surface in the western Sichuan plateau from across the whole Sichuan-Yunnan area, with a maximum uplift rate of approximately 5.8 mm/a, which is equivalent to 1.8×10^{-8} ms^{-2}/a in terms of gravity variation. The results from Hao et al. [25], which were based on leveling observations in the eastern margin of the Tibetan Plateau between 1970 and 2011, also indicated the maximum vertical movement rate to be approximately 5.7 mm/a in the Sichuan-Yunnan area. Thus, the vertical surface movement played an insignificant role in the gravity variation results yielded in this work, and they likely resulted from changes in deep material distribution. From the standpoints of regional geodynamics and deep material properties, the deep material in the study area indeed has the potential of migrating on a large scale. First, there is a consensus that the material at the east margin of the Tibetan Plateau experiences a lateral flow under the combined action of the Indian Plate pushing northward and the Yangtze Plate blocking. The study area is located at the southern-central part of the east margin of the Tibetan Plateau, where the material flow has a critical deflection from eastward to southeastward. Therefore, a geodynamic context is present for such crustal material migration. Second, a low-velocity layer widely exists in the middle to lower crust of the western Sichuan plateau [26–29]. This low-velocity material can experience a large-scale flow or density change under the control of deep tectonic dynamics, thus leading to significant variation in the gravity field.

When comparing our results with those of current studies on horizontal crust movement, we realized that there was reasonable consistency between the gravity variation and crustal motion. According to the crustal movement data acquired by GPS observation [30–33], a most intense horizontal motion took place in the crust in the central Sichuan-Yunnan area, and the predominant moving direction was southeast with a gradual deflection to the south and southwest. The Longmenshan Fault and the Lianfeng, Zhaotong faults in this region had considerable absorption effects for the crustal movement, as the moving rates in the direction normal to the Longmenshan and Lianfeng, Zhaotong fault zones experienced an appreciable decrease across them [32,33]. These features are in accordance with the observations that the positive-anomaly region shifted southeastward in the differential variation patterns, the positive-anomaly region in the western Sichuan plateau expanded southward with the Anninghe Fault as a boundary in the cumulative variation patterns, and the Longmenshan and Lianfeng, Zhaotong faults played a role in governing the boundaries of the spatial distribution of the gravity variation. It is true that gravity variation has marked short-term effects relative to GPS observations. Because gravity variation arises as a composite reflection of changes in deep material distribution while GPS observations record the results of crustal movement at the surface, the differences between them can stem from distinctions in material motion between the surface and at depth. Numerical simulations of lower crust flow in the Sichuan-Yunnan area [34,35] indicated that material in the lower crust of this region flowed more easily than that in the upper crust, thus having a greater flow velocity. This likely caused temporal differences in gravity variation and the geometric deformation that was observed at the surface. If so, migration of deep crust material should have had a more significant effect on the development and occurrence of the Ludian *Ms*6.5 and Kangding *Ms*6.3 strong earthquakes.

6. Conclusion

Surface gravity variation contains rich information about crustal movement and constitutes an important basis for understanding the rules of earthquake development and occurrence and for practicing earthquake predictions. This work used mobile surface gravity measurements in the central area of Sichuan and Yunnan provinces collected between 2013 and 2015, and obtained recent gravity variation patterns in this region. The relationships between the gravity variation and the Ludian *Ms*6.5 earthquake on August 3rd, 2014, and between the gravity variation and the Kangding *Ms*6.3 earthquake on November 22nd, 2014, were studied. We also discussed the mechanisms of the gravity variation in combination with the regional geodynamics context and crustal movement features. The following conclusions were reached:

1) The gravity variation prior to both the Ludian *Ms*6.5 and Kangding *Ms*6.3 earthquakes showed certain characteristics that were in agreement with the “precursor anomalies” found in the Tangshan and Wenchuan earthquakes. Preseismic positive anomalies occurred near the epicenter, and high gradient zones crossed the epicenter before the both earthquakes. Furthermore, deflection of the gradient zone accompanied the gravity variation prior to the Ludian earthquake. Based on these anomalies, GNCC made a relatively accurate prediction of the locations of the two earthquakes.
2) The gravity variation was reasonably consistent with the material migration context and the crust movement observations on the Tibetan Plateau. In the gravity variation patterns, the positive-anomaly regions exhibited a trend that shifted southeast, which matched the direction of the crustal motion that was recorded by GPS observation. The Longmenshan and Lianfeng, Zhaotong faults in this region had an obvious effect on controlling the boundaries of the spatial distribution of the gravity variation, which is in agreement with the absorption effects of the fault zones during the crustal movement.
3) Deep material migration was likely the primary cause of the gravity variation, and it could also have been an important factor in inducing the development and occurrence of the Ludian *Ms*6.5 and Kangding *Ms*6.3 earthquakes.

Acknowledgments

This work is jointly supported by the Director Foundation of Institute of Seismology, China Earthquake Administration (IS201326121), the special earthquake research grant offered by the China Earthquake Administration (201208009, 201308009) and the National Natural Science Foundation of China (41304059).

The data used in this work were acquired by the Hubei Earthquake Administration, Sichuan Earthquake Administration, Yunan Earthquake Administration, First Crust Monitoring and Application Center, China Earthquake Administration and Second Crust Monitoring and Application Center, China Earthquake Administration. They are thanked by the authors.

REFERENCES

[1] Xiwei Xu, Guoyan Jiang, Guihua Yu, Xiyan Wu, Jianguo Zhang, Xi Li. Discussion on seismogenic fault of the Ludian MS6.5 earthquake and its tectonic attribution. Chin J Geophys 2014;57(09):3060–8 [in Chinese].
[2] Yong Zhang, Lisheng Xu, Yuntai Chen, Ruifeng Liu. Rupture process of the 3 August 2014 Ludian, Yunnan, MW6.1(MS6.5) earthquake. Chin J Geophys 2014;57(09):3052–9 [in Chinese].

[3] Chengli Liu, Yong Zheng, Xiong Xiong, Rui Fu, Bin Shan, Faqi Diao. Rupture process of MS6.5 Ludian earthquake constrained by regional broadband seismograms. Chin J Geophys 2014;57(09):3028–37 [in Chinese].
[4] Chaozhong Hu, Panxin Yang, Peng Liang, Peng Su, Renwei Xiong, Xiaoqiang Li, et al. The Holocene paleo earthquakes on the 2014 Kangding MS6.3 earthquake faults. Chin Sci Bull 2015;60(23):2236–44 [in Chinese].
[5] Guixi Yi, Feng Long, Xueze Wen, Mingjian Liang, Siwei Wang. Seismogenic structure of the M6.3 Kangding earthquake sequence on 22 Nov. 2014, Southwestern China. Chin J Geophys 2015;58(04):1205–19 [in Chinese].
[6] Dahu Li, Zhifeng Ding, Pingping Wu, Chen Zheng, Qingdong Ye, Mingjian Liang. The deep seismogenic environment of the southeastern section of Xianshuihe fault zone and the 2014 Kangding MS6.3 earthquake. Chin J Geophys 2015;58(06):1941–53 [in Chinese].
[7] Shi Chen, Qinghua Wang, Qianshen Wang, Yan Wang, Hongyan Lu, Weimin Xu, et al. The 3D density structure and gravity change of Ludian MS6.5 Yunnan epicenter and surrounding regions. Chin J Geophys 2014;09:3080–90 [in Chinese].
[8] Guangliang Yang, Chongyang Shen, Hongbo Tan, Jiapei Wang, Guiju Wu. Crustal density structure of Yunnan Ludian MS6.5 earthquake area. Seismol Geol 2014;04:1145–56 [in Chinese].
[9] Barnes DF. Gravity changes during the Alaska earthquake. J Geophys Res 1966;71(2):451–6.
[10] Fujii Y. Gravity changes in the shock area of the Niigata earthquake, 16 June 1964. Zisin 1966;19(3):200–16.
[11] Hunt TM. Gravity changes associated with the 1968 Inangahua earthquake. N. Z J Geol Geophys 1970;13(4):1050–1.
[12] Kisslinger C. Processes during the Matsushiro, Japan, earthquake swarm as revealed by leveling, gravity, and spring-flow observations. Geology 1975;3(2):57–62.
[13] Chongyang Shen, Hui Li, Shaoan Sun, Shaoming Liu, Songbai Xuan, Hongbo Tan. Dynamic variation of gravity and the preparation process of the Wenchuan Ms8.0 earthquake. Chin J Geophys 2009;52(10):2547–57 [in Chinese].
[14] Yiqing Zhu, Yunma Xu, Yipei Lv, Tieming Li. Relations between gravity variation of Longmenshan fault zone and Wenchuan Ms8.0 earthquake. Chin J Geophys 2009;52(10):2538–46 [in Chinese].
[15] Yiqing Zhu, Fang Liu, Weifeng Liang, Yunma Xu. Gravity variation associated with Wenchuan earthquake in western Sichuan. Geodes Geodyn 2011;2(1):55–60.
[16] Yiqing Zhu, Shusong Guo, Fang Liu. Variation of gravity field before and after Panzhihua Ms6.1 and Yaoan Ms6.0 earthquakes. J Geodes Geodyn 2010;30(4):8–11 [in Chinese].
[17] Yiqing Zhu, Xueze Wen, Heping Sun, Shusong Guo, Yunfeng Zhao. Gravity changes before the Lushan, Sichuan, Ms=7.0 earthquake of 2013. Chin J Geophys 2013;56(6):1887–94 [in Chinese].
[18] Farrell W. Deformation of the Earth by surface loads. Rev Geophys 1972;10(3):761–97.
[19] Yuntai Chen, Haoding Gu, Zaoxun Lu. Variation of gravity before and after the Haicheng earthquake, 1975 and the Tangshan, 1976. Acta Seismol Sinaca 1980;2(1):21–31 [in Chinese].
[20] Ruihao Li, Jianliang Huang, Hui Li, Dongsheng Chen. The mechanism of regional gravity change s before and after the Tangshan earthquake. Acta Seismol Sinaca 1997;19(4):399–407 [in Chinese].
[21] Chongyang Shen, Hui Li, Shaoan Sun, Guangliang Yang, Songbai Xuan, Hongbo Tan, et al. Characteristic analysis of dynamic gravity change before Yutian Ms7.3 earthquake. J Geodesy Geodyn 2008;2010(04):1–7 [in Chinese].
[22] Yiqing Zhu, Shuangxu Wang, Zaisen Jiang, Guizhi Zhu, Hui Li, Yongzhi Zhang. Gravity variation before Kunlun mountain pass western Ms8.1 earthquake. Acta Seismol Sinaca 2003;03:291–7 [in Chinese].
[23] Yiqing Zhu, Weifeng Liang, Feibing Zhan, Fang Liu, Yunma Xu, Shusong Guo, et al. Study on dynamic change of gravity field in China continent. Chin J Geophys 2012;55(3):804–13 [in Chinese].
[24] Qingliang Wang, Duxin Cui, Wenping Wang, Sixin Zhang, Jinwen Liu, Qi Shi. Study on present-day vertical crust movement in western Sichuan area. Sci China Earth Sci 2008;38(5):598–610 [in Chinese].
[25] Ming Hao. Present crustal vertical movement of eastern Tibet plateau and coseismic and postseismic vertical deformation of two typical Earthquake[D]. 2012 [PhD thesis] [in Chinese].
[26] Royden LH, Clark BC, King RW, Erchie W, Zhiliang Chen, Feng Shen, et al. Surface deformation and lower crustal flow in eastern Tibet. Science 1997;276:788–90.
[27] Clark MK, Royden LH. Topographic ooze: building the eastern margin of Tibet by lower crustal flow. Geology 2000;33:525–8.
[28] Burchfiel BC, Chen Zhiliang, Liu Yunping, Royden LH. Tectonics of the Longmen Shan and adjacent regions, central China. International Geology Review 1995;37:661–735.
[29] Haiyan Yang, Jiafu Hu, Hong Zhao, Youjin Su. Crust-mantle structure and seismogenic background of Wenchuan Ms8.0 earthquake in Western Sichuan area. Chin J Geophys 2009;52(2):356–64 [in Chinese].
[30] Xuejun Qiao, Qi Wang, Ruilin Du. Characteristic of current crustal deformation of active blocks in the Sichuan-Yunnan region. Chin J Geophys 2004;47(5):805–11 [in Chinese].
[31] Shen Z-K, Lü J, Wang M, Bürgmann Roland. Contemporary crustal deformation around the southeast borderland of the Tibetan Plateau. J Geophys Res Solid Earth 2005;110(B11409). 2004JB003421.
[32] Liang S, Gan W, Shen C, Xiao G, Liu J, Chen W, et al. Three-dimensional velocity field of present-day crustal motion of the Tibetan Plateau derived from GPS measurements. J Geophys Res Solid Earth 2013;118(10). 2013JB010503.
[33] Xueze Wen, Fang Du, Guixi Yi, Feng Long, Jun Fan. . Earthquake potential of the Zhaotong and Lianfeng fault zones of the eastern Sichuan-Yunnan border region. Chin J Geophys 2013;56(10):3361–72 [in Chinese].
[34] Shoubiao Zhu, Yaolin Shi. Genetic algorithm-finite element inversion of drag forces exerted by the lower crus on the upper crust in the Sichuan-Yunnan area. Chin J Geophys 2004;47(2):232–9 [in Chinese].
[35] Shoubiao Zhu, Yaolin Shi. Genetic algorithm-finite element inversion of topographic spreading forces and drag forces of lower crust to upper crust in Tibet plateau. Acta Scientiarum Naturalium Universitatis Pekinensis 2005;41(2):225–34 [in Chinese].

Hao Hongtao, assistant research at Institute of Seismology, China Earthquake Administration. His current research interests focus on surface gravimetric technology and data processing.